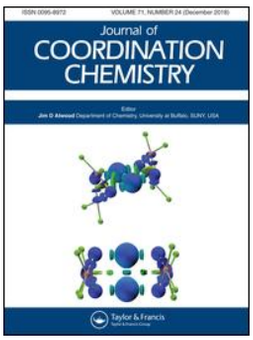

Journal of Coordination Chemistry

ISSN: (Print) (Online) Journal homepage: https://www.tandfonline.com/loi/gcoo20

Cu(II) complexes of hydrazones–NSAID conjugates: synthesis, characterization and anticancer activity

Jatinder Kaur , Tanmayee Chikate , Parbati Bandyopadhyay , Soumya Basu & Rajeev Chikate

To cite this article: Jatinder Kaur , Tanmayee Chikate , Parbati Bandyopadhyay , Soumya Basu & Rajeev Chikate (2020): Cu(II) complexes of hydrazones–NSAID conjugates: synthesis, characterization and anticancer activity, Journal of Coordination Chemistry, DOI: 10.1080/00958972.2020.1843160

To link to this article: https://doi.org/10.1080/00958972.2020.1843160

JOURNAL OF COORDINATION CHEMISTRY
https://doi.org/10.1080/00958972.2020.1843160

Cu(II) complexes of hydrazones–NSAID conjugates: synthesis, characterization and anticancer activity

Jatinder Kaur[a,b], Tanmayee Chikate[c,d], Parbati Bandyopadhyay[b], Soumya Basu[c] and Rajeev Chikate[a]

[a]Department of Chemistry, Post-graduate and Research Center, MES Abasaheb Garware College, Pune, India; [b]Department of Chemistry, Fergusson College, Pune, India; [c]Dr. D. Y. Patil Biotechnology and Bioinformatics Institute, Cancer and Translational Research Laboratory, Pune, India; [d]Department of Bioengineering, University of Texas, Arlington, USA

ABSTRACT

The hydrazones of nonsteroidal anti-inflammatory drugs (NSAIDs) diclofenac and ibuprofen are synthesized with aldehydes of pyridine and imidazole and are characterized by ^{1}H, ^{13}C and mass spectroscopy. Cu(II) complexes of hydrazones constructed from these ligands possess square planar geometry for bidentate diclofenac-hydrazone and tridentate ibuprofen-hydrazone conjugates with $[Cu(L)_2]$ and [Cu(L)Cl] compositions, respectively. The observed irreversible Cu(II)/Cu(I) redox couple in the range of +0.20 to +0.61 V is due to the substantial distortion in the square-planar geometry. ESR studies indicate the appreciably covalent character within M–L bonding due to extensive delocalization of electron from $d_{x^2-y^2}$ orbital. The hydrazone–NSAID conjugates exhibit substantial cytotoxicity against A-549, HCT-116 and MDA-MB-231 cancer cell lines with ibuprofen-imidazole-hydrazone ligand possessing the lowest IC_{50} (2.26 μM) amongst the synthesized NSAID-conjugates. Interestingly, its Cu(II) complex also displays excellent anticancer activity against MDA-MB- 231 with IC_{50} value of 3.58 μM. Such a feature may be ascribed to the synergistic association of Cu(II)–NSAID–hydrazone linkage. Thus, conjugation of NSAID with hydrazone and its complexation with a bioactive metal ion may be regarded as a potential strategy for designing of non-platinum anticancer agents.

ARTICLE HISTORY
Received 21 July 2020
Accepted 13 October 2020

KEYWORDS
Cu(II) complexes; aroyl hydrazones; NSAID; anticancer activity; ESR; cyclic voltammetry

CONTACT Rajeev Chikate rajuchikate29@gmail.com, rajeev.chikate@mesagc.org Department of Chemistry, Post-graduate and Research Center, MES Abasaheb Garware College, Pune, India.

Supplemental data for this article is available online at https://doi.org/10.1080/00958972.2020.1843160.

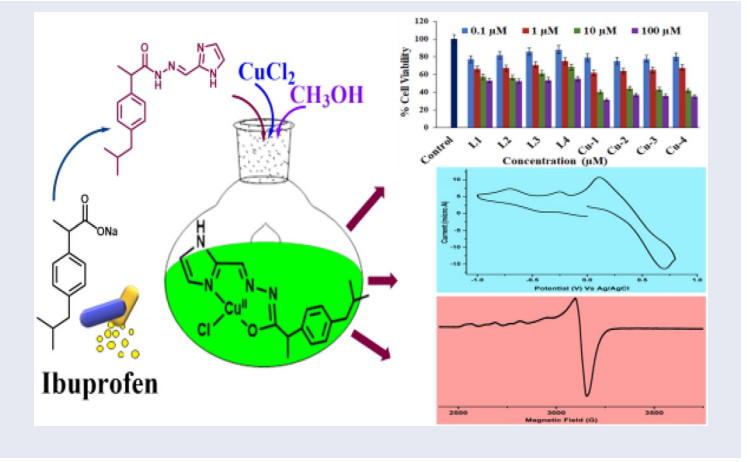

1. Introduction

Nonsteroidal anti-inflammatory drugs (NSAIDs) consist of analgesic, antithrombotic antipyretic and anti-inflammatory agents that are commonly employed for the treatment of arthritis, spondylitis and ocular conditions for several decades [1–3]. The anti-inflammatory activity of NSAIDs is attributed to its irreversible inhibition of cyclo-oxygenase enzymes like COX-1 and COX-2 [4,5]. COX-1 is primarily responsible for "housekeeping" functions of tissues while COX-2 is expressed as a response towards tissue injuries for catalyzing the conversion of arachidonic acid to prostaglandins and thromboxane that are responsible for inflammation and mitogenesis of tissues and cells [6,7]. Interestingly, several epidemiologic and clinical investigations have suggested the chemopreventive and cytotoxic potency of NSAIDs against different types of cancers like colon, breast, lung, gastric and prostate [8–15]. Diclofenac, a nonsteroidal anti-inflammatory drug, exhibits enhanced ROS production and lowers the mitochondrial superoxide dismutase levels to exert cytotoxicity on human melanoma cell line A2058 [16]. Another compound of this class, ibuprofen, when administered in combination with cisplatin, improved the suppression of overexpressed Hsp70 protein in lung cancer cell line that triggers the mitochondrial apoptosis [17]. On the other hand, aspirin; an anti-pyretic and anti-inflammatory drug, suppresses the propagation of cervical cancer cell (HeLa) and induces apoptosis through inhibition of proto-oncogene (ErbB2) signaling pathway [18]. Thus, cytotoxic behavior of NSAIDs is attributed to a variety of mechanistical processes such as inhibition of COX-2 enzyme, inhibition of angiogenesis, disrupting glucose metabolism, blocking signal transduction pathways and triggered apoptosis [19–26].

In spite of possessing significant anticancer activity, the potentiality of NSAIDs as antitumor drugs is remained unexplored due to their anionic nature under physiological pH as well as restricted binding to polyanionic DNA. It accounts for excessive accumulation in cancer cells and causes considerable cytotoxic effects. To overcome this lacuna, one of the approaches is adopted where these anionic motifs are coordinated to transition metal ions so as to form stable complexes. It is speculated that

hydrophobic and lipophilic NSAID facilitates the transport of metal complex through lipophilic cell membrane that ultimately binds to cellular components of cancer cells and subsequently triggers either necrosis or apoptosis of infectious cells [27]. Exploring this hypothesis, a variety of metal complexes of NSAID synthesized with different metals such as Ag, Pt, Ru, Os, Cu, Co are found to exhibit significant antitumor activity [28,29]. For instance, Cu(II) complex of aspirin is found to be 30 times more potent than aspirin while similar observations are noted for the diclofenac complex $[Cu(diclofenac)_2(H_2O)_2]\cdot 2H_2O$ that exhibits substantial cytotoxic behaviour against human colon adenocarcinoma, SW620 and HT29 cell lines. These features are also reported for Cu(II)-ibuprofen complex that displayed better anticancer activity towards human melanoma as compared to ibuprofen [30–34].

To further enhance the activity of NSAIDs, another strategy is envisaged that involves condensation of these scaffolds with heterocyclic aldehydes/ketones and these functionalized NSAID may enhance the cytotoxicity, preferential binding with DNA and subsequently improves the bio-activity of NSAIDs [35]. For this purpose, hydrazones derived from the anti-inflammatory agents are synthesized as it is well documented that hydrazones possess excellent biological activities towards a variety of disorders, including cancer [36]. Also, they exhibit beneficial coordination capability as ligands towards different metal ions and these complexes are found to be more active than hydrazones . Thus, it is imperative to construct the metal-based NSAIDs-hydrazone conjugates as an alternative to toxic platinum-based anticancer agents that may exhibit better anti-proliferative activity with lower IC_{50} values [37].

With these objectives, we have constructed hydrazones of anti-inflammatory drugs like diclofenac and ibuprofen that are derived from their respective hydrazides and heterocyclic aldehydes. The synthesized Schiff base ligands are further utilized for the formation of Cu(II)-conjugates having empirical formulas as $[Cu(L)_2]$ and [CuLCl] for hydrazones of diclofenac and ibuprofen, respectively. These motifs are evaluated for the anticancer activity against breast adenocarcinoma (MDA MB-231), adenocarcinomic human alveolar basal epithelial (A549) and colorectal carcinoma (HCT116) cancer cell lines.

2. Experimental

2.1. Materials and methods

A.R. grade chemicals were used as received. Hydrazine hydrate, pyridine-2-aldehyde, imidazole-2-carboxaldehyde and copper(II) chloride were procured from Aldrich. Sodium salt of diclofenac and ibuprofen hydrochloride were a generous gift from a pharmaceutical company and used only for academic purpose. Tetraethylammonium perchlorate (TEAP) used for electrochemistry was prepared as reported. Triple negative breast adenocarcinoma (MDA MB-231), adenocarcinomic human alveolar basal epithelial (A-549) and colorectal carcinoma (HCT-116) cell lines were procured from the National Centre for Cell Science (NCCS), Pune, India. Reagents like L-glutamine (200 mM), antibiotic and antimyotic reagents (100X), trypsin (0.25%), EDTA (0.02%), phosphate buffered saline (PBS), fetal bovine serum (FBS), Dulbecco's modified Eagle medium (DMEM), MCoy-5A medium, F-12K media and MTT (3-[4,5-dimethyl-2-thiazole]-2,5-diphenyl-2*H*-tetrazolium) were purchased from Hi-Media. Triton X-100, isopropanol

and HCl were obtained from Qualigens. HPLC grade (Aldrich) deuterated solvents $CDCl_3$ (99.9%), D_2O (99.9%) and DMSO-d_6 (99.5%) were employed for spectroscopic analysis. Other solvents like methanol, acetonitrile, diethylether, dimethylsulfoxide (DMSO) and dimethylformamide (DMF) were purified and dried before use as per established protocol. Triply distilled water was used for the biochemical studies.

2.2. Synthesis of ligands (L_1–L_4)

2.2.1. Synthesis of diclofenac hydrazide (DHZ) and ibuprofen hydrazide (IHZ)

The hydrazides of diclofenac and ibuprofen were prepared as per the literature reports [38,39]. The sodium salt of diclofenac/ibuprofen (10 mmol) was refluxed in methanol (20 mL) with a catalytic amount of H_2SO_4 for 6 h so as to obtain its methyl ester. The white solid obtained was filtered and washed with $NaHCO_3$ (5%). The methyl ester was refluxed with hydrazine hydrate (99%) in methanol for 4 h. The solid mass was filtered, recrystallized from methanol and dried under vacuum. The hydrazides of diclofenac and ibuprofen were abbreviated as DHZ and IHZ, respectively. The ^{1}H NMR (Figure S1) and elemental analysis data of DHZ and IHZ is as follows:

DHZ: ^{1}H NMR, δ (ppm), ($CDCl_3$): 3.68 (3.81, 2H, 2 s, CH_2CO), 4.21 (2H, s, NH_2), 6.60-7.37 (7H, m, aromatic), 7.64 (1H, s, NH), 8.58 (1H, s, -CONH). Elemental analysis: $C_{14}H_{13}Cl_2N_3O$ (%) Calc.: C, 54.21; H, 4.22; Cl, 22.86; N, 13.55. Found: 54.28; H, 4.12; N, 13.36.

IHZ: ^{1}H NMR, δ (ppm), ($CDCl_3$): 0.86 (0.88*, d, 6H, –$(CH_3)_2$), 1.52 (1.25*, d, 3H, –CH_3CH), 1.81-1.87 (m, 1H, –CH$(CH_3)_2$), 2.44 (2.45*, 2H, –CH_2Ar), 3.52 (3.51*, q, 1H –$CHCH_3$), 3.83 (s, 2H, –NH_2, D_2O exchangeable), 6.26 (6.68*, s, 1H, –CONH, D_2O exchangeable), 7.10–7.12 (d, 2H, aromatic), 7.17–7.19 (d, 2H, aromatic). Elemental analysis: $C_{13}H_{20}N_2O$ (%) Calc.: C, 70.87; H, 9.15; N, 12.72. Found: C, 70.84; H, 9.23; N, 12.62.

2.3. Synthesis of hydrazone of DHZ and IHZ

DHZ (10 mmol) was treated with pyridine-2-aldehyde (10 mmol) in 20 mL methanol with a drop of acetic acid and the resulting solution was refluxed for 6 h under constant stirring. White solid was filtered, washed with cold methanol and recrystallized form methanol. This ligand was abbreviated as **L_1**. Similar procedure was adopted for the synthesis of other ligands with IHZ and imidazole-2-carboxaldehyde which were abbreviated as **L_2**–**L_4**. The single-crystals of **L_4** were grown by slow evaporation of mother liquor of reaction mixture. The spectroscopic data for **L_1**–**L_4** are as follows:

L_1: 2-(2-((2,6-dichlorophenyl)amino)phenyl)-*N*′-(pyridin-2-ylmethylene)acetohydrazide: Yield: 85%; Elemental analysis: $C_{20}H_{16}Cl_2N_4O$ (%) Calc.: C, 60.16; H, 4.04; N, 14.09. Found: C, 60.21; H, 4.06; N, 13.99. ^{1}H NMR, δ (ppm), (DMSO-d_6): 4.16 (3.74*, s, 2H, –CH_2), 7.65 (s, 1H, –NH, D_2O exchangeable), 8.11 (8.26*, s, 1H, –N = CH), 6.27–8.62 (m, 12H, aromatic and azomethine), 11.82 (12.07*, s, 1H, –CONH, D_2O exchangeable). ^{13}C NMR, δ (ppm), (DMSO-d_6): 36.02 (38.74*, –CH_2), 116.07-150.02 (aromatic carbons), 153.35 (153.39*, –C = N), 173.11 (168.56*, –CONH). IR ($cm^{-(}$): 3308 ν(N–H), 1645 ν(C = O), 1566 ν(C = N), 1499 $\nu(C=N)_{heterocyclic}$. ESI MS: 399.078 $[M+H]^+$, 421.06 $[M+Na]^+$ (Figure S2).

L_2: *N′*-((1*H*-imidazol-2-yl)methylene)-2-(2-((2,6-dichlorophenyl)amino)phenyl)acetohydrazide: Yield: 88%; Elemental analysis: $C_{18}H_{15}Cl_2N_5O$ (%) Calc.: C, 55.68; H, 3.89; N, 18.04. Found: C, 55.57; H, 3.80; N, 18.08. ^{1}H NMR, δ (ppm), (DMSO-d_6): 4.19 (3.72*, s, 2H, –CH_2), 7.84 (s, 1H, –NH, D_2O exchangeable), 6.30–7.55 (m, 9H aromatic) 8.14 (7.95*, s, 1H, –N = CH), 11.48-12.90 (bs, 2H, –CONH and –$NH_{imidazole}$, D_2O exchangeable). ^{13}C NMR, δ (ppm), ppm (DMSO-d_6): 35.62 (38.86*, –CH_2), 116.31–142.99 (aromatic carbons), 143.43 (143.66*, –C = N), 173.71 (168.32*, –CONH). IR ($cm^{-(}$): 3250 ν(N–H), 1661 ν(C = O), 1564 ν(C = N), 1502 $\nu(C=N)_{heterocyclic}$. ESI MS: 388.07 $[M+H]^+$, 410.05 $[M+Na]^+$ (Figure S3).

L_3: 2-(4-Isobutylphenyl)-*N′*-(pyridin-2-ylmethylene)propanehydrazide: Yield: 88%; Elemental analysis: $C_{19}H_{23}N_3O$ (%) Calc.: C, 73.76; H, 7.49; N, 13.58. Found: C, 73.43; H, 7.35; N, 13.31. ^{1}H NMR, δ (ppm), ($CDCl_3$): 0.85 (0.87*, d, 6H, –$(CH_3)_2$), 1.54 (1.58*, d, 3H, –CH_3CH), 1.78–1.84 (m, 1H, –CH$(CH_3)_2$), 2.40 (2.43*, 2H, –CH_2Ar), 4.70 (3.69*, q, 1H –$CHCH_3$), 7.07–8.59 (s, 8H, aromatic and azomethine), 9.85 (9.47*, s, 1H, –CONH, D_2O exchangeable). ^{13}C NMR, δ (ppm), ($CDCl_3$): 18.42 (18.60*, –CH_3), 22.39(22.41*, (–$CH_3)_2$), 30.16 (–$CHCH_2$), 41.35 (–CH_2), 45.05 (45.59*(–$CHCH_3$), 120.16–149.14 (aromatic carbons), 153.21 (152.82*, –C = N), 176.86 (171.19*, –CONH). IR ($cm^{-(}$): 3396 ν(N–H), 1661 ν(C = O), 1552 ν(C = N), 1511 $\nu(C=N)_{heterocyclic}$. ESI MS: 388.07 $[M+H]^+$, 410.05 $[M+Na]^+$ (Figure S4).

L_4: *N′*-((1*H*-imidazol-2-yl)methylene)-2-(4-isobutylphenyl)propanehydrazide: Yield: 90%; Elemental analysis: $C_{17}H_{22}N_4O$ (%) Calc.: C, 68.43; H, 7.43; N, 18.78. Found: C, 68.29; H, 7.23; N, 18.64. ^{1}H NMR, δ (ppm), (DMSO-d_6): 0.83 (0.85*, d, 6H, (–$CH_3)_2$), 1.38 (1.40*, d, 3H, –CH_3), 1.76–1.83 (m, 1H, –CH$(CH_3)_2$), 2.37 (2.40*, 2H, –CH_2Ar), 4.85 (3.63*, q, 1H, –$CHCH_3$), 7.05–7.35 (m, 6H, aromatic), 7.86 (8.10*, s, 1H, –N = CH), 11.25 (11.53*, s, 1H, –CONH, D_2O exchangeable), 12.65 (bs, 1H, –$NH_{imidazole}$, D_2O exchangeable). ^{13}C NMR, δ (ppm), (DMSO-d_6): 18.54 (19.02*, –CH_3), 22.65 (22.69*, $(CH_3)_2$), 30.04 (30.10, –$CHCH_2$), 39.25 (–CH_2), 44.70 (44.19*, –$CHCH_3$), 127.46–140.08 (aromatic carbons), 142.83 (143.12*, C = N), 175.76 (170.29*, –CONH). IR ($cm^{-(}$): 3233 (νN–H), 1665 ν(C = O), 1550 ν(C = N), 1513 $\nu(C=N)_{heterocyclic}$. ESI MS: 299.18 $[M+H]^+$, 321.16 $[M+Na]^+$ (Figure S5).

2.4. Synthesis of copper(II) complexes

To a methanolic solution of **L_1** (161 mg, 0.5 mmol), copper(II) chloride (85 mg, 0.5 mmol) dissolved in methanol was added dropwise and the mixture was stirred for 6 h. The green solid obtained was filtered, washed with water, followed by diethylether and dried under vacuum. The obtained copper complex was abbreviated as **Cu-1**. Similar procedure was followed for synthesis of **Cu-2**, **Cu-3** and **Cu-4** with **L_2**, **L_3** and **L_4**, respectively. The spectroscopic data for **Cu-1**–**Cu-4** are as follows:

Cu-1: $[Cu(L_1)_2]$; Yield: 48%; IR (KBr pellet, cm^{-i}): 3313, 1601; ESI-MS (*m/z*, (%) positive mode): 882.0417 $[M+Na]^+$, 860.0611 $[M+H]^+$, 461.9893 $[M\text{-}L_1+H]^+$, 799.1451 $[L_1 + L_1 + H]^+$, 821.1127 $[L_1 + L_1 + Na]^+$ (Figure S6); UV–vis (DMSO), λ_{max} (nm), ε ($M^{-(M}cm^{-1}$): 282 (15600), 360 (11540), 744 (194); Anal. Calcd. for $CuC_{40}H_{30}Cl_4N_8O_2$ (%): C, 55.86; H, 3.52; N, 13.03. Found: C, 55.84; H, 3.46; N, 13.12.

Cu-2: $[Cu(L_2)_2]$; Yield: 45%; IR (KBr pellet, cm^{-i}): 3317, 1597; ESI-MS (*m/z*, (%) positive mode; 838.05 $[M+H]^+$, 451.99 $[M\text{-}L_2{+}H]^+$, 777.13 $[L_2{+}L_2{+}H]^+$, 799.12 $[L_2{+}L_5{+}Na]^+$ (Figure S7); UV–vis (DMSO), λ_{max} (nm), ε ($M^{-(M}cm^{-1}$): 284 (17800), 370 (11700), 790 (226); Anal. Calcd. for $CuC_{36}H_{28}Cl_4N_{10}O_2$ (%): C, 51.60; H, 3.37; N, 16.71; Found: C, 51.45; H, 3.12; N, 16.67.

Cu-3: $[Cu(L_3)Cl]$; Yield: 52%; IR (KBr pellet, cm^{-C}): 3249, 1621; ESI-MS (*m/z*, (%) positive mode): 407.08 $[M+H]^+$, 449.12 $[M+DMSO\text{-}Cl]^+$, 372.11 $[M\text{-}Cl]^+$ (Figure S8); UV–vis (DMSO), λ_{max} (nm), ε ($M^{-(M}cm^{-1}$): 287 (14160), 373 (21400), 775 (226); Anal. Calcd. for $CuC_{19}H_{22}N_3OCl$ (%): C, 56.02; H, 5.44; N, 10.31; Found: C, 55.99; H, 5.49; N, 10.23.

Cu-4: $[Cu(L_4)Cl]$ Yield: 53%; IR (KBr pellet, cm^{-C}): 3210, 1598; ESI-MS (*m/z*, (%) positive mode): 438.11 $[M+DMSO\text{-}Cl]^+$, 361.11 $[M\text{-}Cl+H]^+$ (Figure S9); UV–vis (DMSO), λ_{max} (nm), ε ($M^{-(M}cm^{-1}$): 317 (10760), 364 (19760); Anal. Calcd. for $CuC_{17}H_{21}N_4OCl$ (%): C, 51.51; H, 5.34; N, 14.13; Found: C, 51.43; H, 5.30; N, 14.08.

2.5. Characterization

The elemental analysis was carried out with a Thermo Finnigan FLASH EA 1112 series C, H, N elemental analyzer. Conductivity measurements were performed on a Digital Conductivity Meter (Systronics, Model 304) whereas room-temperature magnetic moments were measured on a Faraday magnetometer, Quantum Design, USA. Electronic spectra of complexes in DMSO were recorded on a Lambda 25, Perkin-Elmer spectrophotometer while infrared spectra were recorded on a Bruker FT-IR spectrophotometer from 4000 to 400 cm^{-1} using KBr pellets. ^1H and ^{13}C NMR spectra were recorded in DMSO-d^6 on a Bruker Ultrashield (400 MHz) and Bruker Avance III HD NMR (500 MHz) spectrometer. The electrospray mass spectra were obtained on a Bruker IMPACT HD mass spectrometer at CIF Department of Chemistry, SPPU using DMSO/methanol as solvent and ESI capillary voltage of 3.5 kV. A CH-1106A potentiostatat was used for cyclic voltammetric measurements of complexes in DMSO containing 0.1 M TEAP as supporting electrolyte. Three-electrode system comprised platinum as working and auxiliary electrode and Ag-AgCl/saturated KCl as reference electrodes. The potentials were calibrated against the ferrocene/ferrocenium couple. X-band ESR spectra in DMSO at 77 K were recorded on a JES-FA200 ESR spectrometer with TCNE as the internal standard at the Sophisticated Analytical Instrument Facility (SAIF), Indian Institute of Technology, Powai, Mumbai.

2.6. Anticancer activity

The cell lines HCT-116, A-549 and MDAMB-231 were maintained in MCoy-5A, F-12K and DMEM media, respectively, with 10% FBS, 1% antibiotic and antimycotic reagent. The cells were cultured in a corning flask and incubated in humidified air containing 5% CO_2 at 37 °C in a CO_2 incubator. On reaching 70% confluency, the media was carefully removed from the flask and 3–5 mL of Trypsin-EDTA was added to detach the adherent cells. The cells were incubated at 37 °C for 4–5 min to facilitate the detachment and then observed under an inverted microscope. Finally, 6–7 mL of media was

added to the flask and the cell suspension was centrifuged at 2000 rpm for 5 min. Subsequently, the supernatant was discarded and the cell pellet was resuspended in fresh growth medium and used for sub-culturing or assay. The cell viability studies with these cell lines were determined by MTT assay [40]. In brief, 100 μL of the cells were seeded in the 96-well plate and incubated for 24 h at 37 °C in a humidified incubator at 5% CO_2. The cell density of 3×10^3 cells/mL was used for seeding of HCT116, A549 and MDAMB-231. After the initial incubation, cells were treated with ligands and their copper complexes at varying concentrations ranging from 100 μM to 0.1 μM in DMSO. After incubation period of 24 h, 10 μL of MTT was added to the cells so as to achieve final concentration of 0.5 mg/mL. The cells were then incubated at 37 °C in the dark for 3 h and subsequently MTT was removed and washed carefully with PBS to remove the traces. The formazan dye formed by action of mitochondrial dehydrogenase was dissolved by incubating the cells in 100 μL of 10% Triton X100 in acidified isopropanol (0.1 N HCl). The absorbance of the purple dye was measured at 570 nm in an ELISA plate reader (Thermofischer Scientific). Simultaneously the untreated cells were maintained as control. The cell viability was calculated for different treatments in relation with negative control taken as 100% viability. All the experiments were conducted in triplicates and at least three different sets of experiments were performed.

2.7. Statistical analysis

All *in vitro* experiments were performed in triplicates and repeated thrice. The data has been presented as mean ± SD. Statistical significance for each variable was estimated by using one-way ANOVA analysis of variance, wherever appropriate. Nonlinear regression was used to determine the IC_{50} values of ligands and their copper complexes by using Graph-pad prism 6 software. The IC_{50} values were interpreted with 95% CI and statistical significance of $p < 0.001$.

3. Results and discussion

3.1. Structural characterization of Cu(II) complexes

The interaction of **L_1–L_4** with copper(II) chloride froms two different types of complexes as proposed in Figure 1. For example, hydrazones of diclofenac possess $[Cu(L)_2]$ stoichiometry with bidentate nature of **L_1** and **L_2** while the corresponding ibuprofen derivatives (**L_3** and **L_4**) generates complexes with 1:1 metal:ligand ratio having composition as [CuLCl] where these ligands behave in a tridentate manner (Table S1). These prepositions are based on the elemental analysis and mass spectra of **Cu-1** to **Cu-4**. Mass spectra (Figures S6 and S7) of **Cu-1** and **Cu-2** suggest the presence of molecular ion $[(M + H)^+]$ peak at 860.06 and 838.05 respectively which corresponds to $[ML_2]$ composition. On the other hand, a peak at 407.08 for **Cu-3** represents the formation of [MLCl] species (Figure S8) while **Cu-4** displays a peak at 438.1147 corresponding to $[M + DMSO\text{-}Cl]^+$ ion (Figure S9). Thus, **Cu-1** and **Cu-2** possess $[ML_2]$ composition while only one ligand is bound to Cu(II) ion with [MLCl] arrangement for **Cu-3** and **Cu-4**. These complexes are non-electrolytic in nature, indicating that chloride ion is coordinated to Cu(II) ion for **Cu-3** and **Cu-4** as well as infer four-coordinate

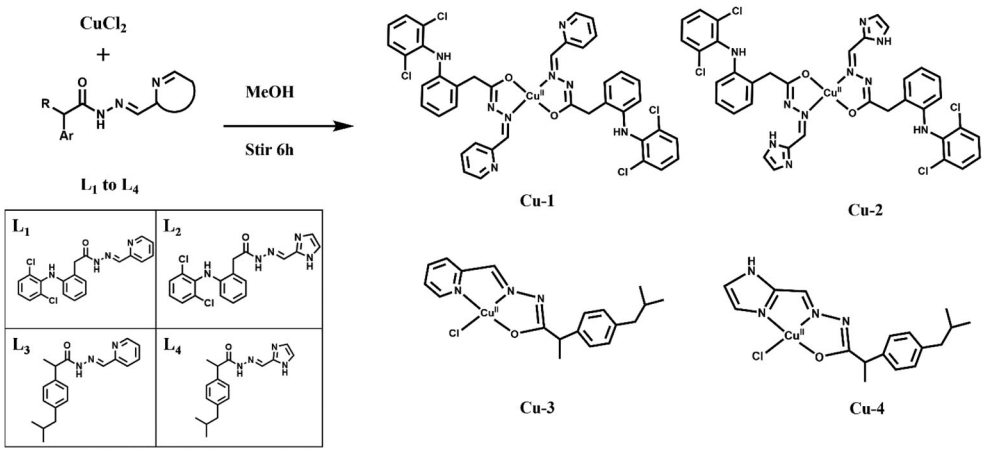

Figure 1. Schematic representation of hydrazones of diclofenac and ibuprofen and their Cu(II) complexes.

geometry for these complexes. The room temperature magnetic moments for these complexes (1.72–1.94 BM) correspond to the square-planar geometry with slight deviation boserved for **Cu-3** and **Cu-4** from the spin-only value (Table S1) indicates the mixing-in effects due to effective low symmetry [41]. The hydrazones of diclofenac bind through enolate oxygen of amide linkage as well as imine nitrogen in a mono-negative bi-dentate manner. However, $\mathbf{L_3}$ and $\mathbf{L_4}$ coordinate with Cu(II) ion *via* hydroxyl oxygen, imine nitrogen and imidazolyl nitrogen in a tridentate manner.

3.2. Spectral analysis

The absorption spectra of copper complexes (Figure S10) exhibit two absorption bands corresponding to ligand based π–π^* and metal to ligand charge transfer (MLCT) transitions in the regions 280–320 and 360–380 nm respectively (Table S2). The metal-based d–d transition appearing as broad peak at lower energy (750–790 nm) is assigned to $^2B_{1g} \rightarrow {}^2B_{1g}$ transition originating from distorted square-planar geometry. Such a behavior probably reflects the presence of unsymmetrical ligand field generated by hydrazone ligands around Cu^{2+} ion for these complexes [41]. Among these complexes, **Cu-1** and **Cu-3** seem to exhibit better resolved bands, probably due to the presence of pyridine ring [42,43].

The disappearnce of $\nu(C=O)_{amide}$ stretching vibration observed in the range of 1645-1672 cm^{-1} for $\mathbf{L_1}$–$\mathbf{L_4}$ (Figure S11) upon complexation with Cu(II) ion implies that this linkage has undergone enolization to generate –OH functionality which after deprotonation binds through hydroxyl oxygen for **Cu-1** to **Cu-4**. The imine nitrogen band $\nu(C=N)$ for the ligands in the region 1550–1566 cm^{-1} is shifted to lower energy side (1485–1510 cm^{-1}) due to the coordination of azomethine nitrogen [44] to Cu(II) ion (Table S3). Interestingly, the difference in the coordination behavior for diclofenac and ibuprofen ligands is observed for heterocyclic nitrogen functionality. For example, vibrational band corresponding to ring nitrogen for $\mathbf{L_1}$ and $\mathbf{L_2}$ remains unaltered after complexation with Cu(II) while this peak for $\mathbf{L_3}$ and $\mathbf{L_4}$ has undergone considerable

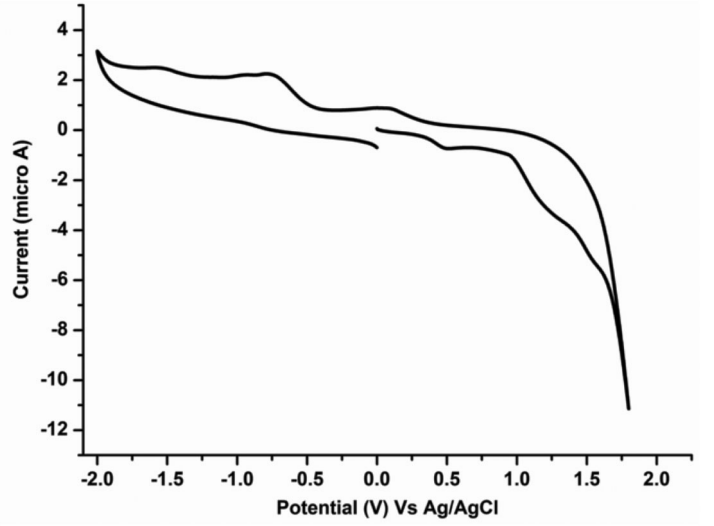

Figure 2. Cyclic volammogram of **Cu-1** at scan rate of 0.1 Vs^{-1}.

lowering by $\sim$ 50 cm^{-1} for **Cu-3** and **Cu-4**. It suggests that hydrazones of diclofenac binds through hydroxyl oxygen and imine; the corresponding hydrazones of ibuprofen coordinated with Cu(II) ion acts as tridentate ligand *via* hydroxyl oxygen, imine and heterocyclic nitrogen atoms. Such a behaviour for the difference in the binding modes probably originates from the structural bulkiness of diclofenac ring that significantly hinders the orientation of hydrazone linkage for the coordination of heterocyclic nitrogen with metal ion. On the other hand, this restriction does not exist for ibuprofen scaffold as it is fairly planar which allows the hydrazone linkage to remain in a planar fashion so that the ligand can effectively bind with three potential donor atoms.

3.3. Electrochemistry

The electrochemical behavior **Cu-1** to **Cu-4** is evaluated in DMSO solvent at a scan rate of 0.1 V s^{-1} and the representative voltammogram is depicted in Figure 2. It is observed that these complexes exhibit several irreversible reduction peaks on cathodic scans (Table 1). For example, peaks in the range of $-$ 0.24 to $-$ 1.50 V are attributed to the reduction of azo (N = N) and imine (C = N) functionality respectively [45] while metal-based Cu(II)/Cu(I) redox couple is observed in the range of +0.20 to +0.61 V. The irreversible nature for Cru(II) redox couple (Figure S12) probably arises due to a distortion in the planar geometry of **Cu-1** to **Cu-4**. It is reported that Cu(II)/Cu(I) couple experiences some structural reorganization due to rearrangement in the geometry form square-planar Cu(II) species to pseudo-tetrahedral Cu(I) moiety [41]. This facet is further correlated to the chemical equilibrium between these two geometries which is primarily responsible for departure from one electron reversible process. Other factors that contribute to such behavior are: (i) stability of Cu(I) species and (ii) presence of π-acceptor ligands. Based on HSAB concept, Cu(II)/Cu(I) couple is shifted towards more positive potential for softer ligands while this peak is observed at more negative

Table 1. Electrochemical data of **Cu-1** to **Cu-4** in DMSO.

Complex	E^0_{red}/V (ΔE_p/mV) values
Cu-1	0.61 (ir), −0.24, −0.70
Cu-2	0.47 (ir), −0.32, −0.81
Cu-3	0.45 (ir), −0.76, −1.50
Cu-4	0.20 (ir), −0.94

potential for hard ligands. This difference may be attributed to the efficient reversible flow of electrons from metal to ligand for softer ligands whereas opposite feature is noted for hard ligands due to higher electronegative character. Thus, more covalent character is present between M–L bonding for soft ligands as against the strong ionic nature for hard ligands. As a consequence of the bonding nature, there exists structural deviation from the square-planar to tetrahedral geometry for these complexes. It is quite likely that **L_1–L_4** possess softer character that induces the structural reorganisation of Cu(II) complexes. These facts can be further corroborated with unequal peak currents for cathodic andanodic scan and ΔE_p (Ep_c-Ep_a) value (>100 mV s^{-1}). Thus, it is quite likely that steric as well as the bulkiness of diclofenac and ibuprofen scaffolds significantly influence the redox behaviour of these complexes and probably induce structural deformity within square-planar geometry for **Cu-1** to **Cu-4** [46,47].

3.4. ESR studies

The magnetically non-diluted polycrystalline X-band ESR spectra of **Cu-1** to **Cu-4** exhibit unsymmetrical nature (Figure 3) with $g_{||}$ and $g_{\perp}$ components originating from planar and axial ligand fields. The EPR spectral g tensors, $g_{||}$ and $g_{\perp}$, are obtained using the equation:

$$g = h\nu/(\beta H)$$

where h is the Planck constant, β is the Bohr magneton, ν is the microwave frequency and H is the applied magnetic field. These complexes exhibit characteristic four peak pattern originating from −3/2, −1/2, +1/2 and +3/2 transitions ($\Delta M_s = \pm 1$) due to Cu-hyperfine interactions ($I = 3/2$) [45, 48]. The $g_{||}$ and $g_{\perp}$ values are 2.30 and 2.07, respectively (Table 2) while g_{av} is found to be significantly higher than free unpaired electron ($g = 2.0023$) value. Moreover, $g_{||} > g_{\perp}$ clearly suggests that the ligands are oriented in planar fashion so as to generate square-planar geometry for these complexes. It also demonstrates that there exists appreciable covalent character for metal-ligand bonding due to significant dπ–pπ interaction between unpaired electron present in metal d-orbital and the empty π-orbital of ligand [49]. It is reported that the unpaired electron is present in the $d_{x^2-y^2}$ orbital of square-planar Cu(II) complexes with significant axial distortion due to strong in plane σ-bonding nature [50] . To ascertain this fact, another parameter *viz.* α^2 (molecular orbital coefficient) is evaluated from the following equation:

$$\alpha^2 = {}^{Cu}A_{||}/P + \left(g_{||} - 2.0023\right) + 3/7\left(g_{\perp} - 2.0023\right) + 0.04$$

where ${}^{Cu}A_{||}$ denotes hyperfine interaction due to copper ion (coupling constant in cm^{-1}) and P is free ion dipolar term (0.036 cm^{-1}). This value also reflects the extent of ionic/covalent character with $\alpha^2 = 1.0$ signifies the ionic while 0.5 corresponds to

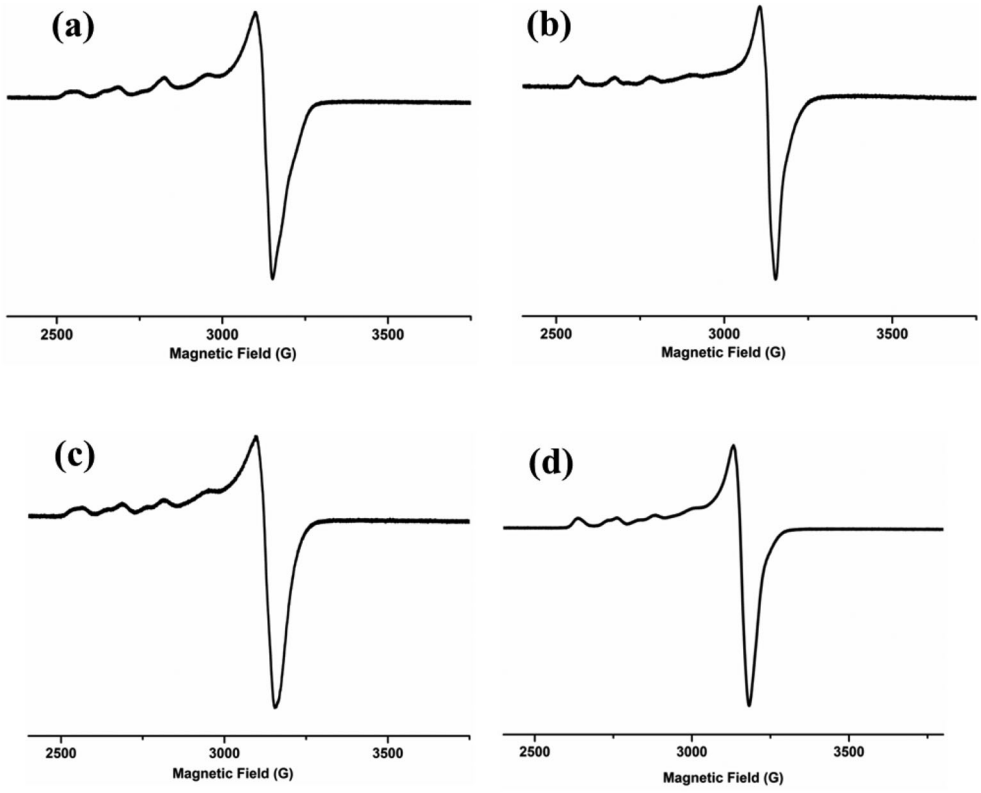

Figure 3. ESR spectra of (a) **Cu-1**, (b) **Cu-2**, (c) **Cu-3** and (d) **Cu-4** at 77 K.

strong covalent character in metal-ligand bonding. For these complexes, these values are found to be in between 1.0 and 0.5 indiating the presence of appreciable covalent character for in plane σ-bonding between $d_{x^2-y^2}$ orbital of metal and ligand π-orbitals [51].

This observation is further corroborated with Cu-hyperfine coupling constant ($^{Cu}A_{||}$) which is significantly lower than observed for perfectly square planar geometry for Cu(II) complexes [52]. Such feature may be ascribed to extensive delocalization of unpaired electronwithin the chelate rings that are formed from bi- or tri-dentate ligands . Moreover, it is quite likely that the extent of delocalization has induced significant covalent character for M–L bonding. The degree of distortion $f(\alpha)$ is calculated by the following equation:

$$f(\alpha) = \left(g_{||}/A_{||}\right)$$

For idealised square planar complex, $f(\alpha)$ value is in between 110- 120 cm^{-1} while moderate distortion exists with 130–150 cm^{-1} and significant distortion [53] is noted when f(α) is in the range of 180–250 cm^{-1}. Inspection of Table 2 reveals that **Cu-1** to **Cu-4** possess substantial distortion from square planar geometry with Cu(II) complexes of ibuprofen exhibiting higher degree of distortion as compared to complexes of diclofenac. This behavior may be attributed to: (i) binding of two bidentate diclofenac ligands ($\mathbf{L_1}$ and $\mathbf{L_2}$) induces the planarity within the structure through linear hydrazone

Table 2. ESR parameters of **Cu-1** to **Cu-4**.

Complex	$g_{\|\|}$	$g_{\perp}$	g_{av}	$A_{\|\|} \times 10^{-4}$ (cm^{-1})	α^2	G	$f(\alpha)$ cm^{-1}
Cu-1	2.32	2.07	2.15	136	0.76	4.57	169
Cu-2	2.31	2.07	2.15	129	0.72	4.42	171
Cu-3	2.31	2.07	2.15	127	0.72	4.42	182
Cu-4	2.30	2.06	2.14	125	0.70	5.0	184

linkage, (ii) coordination of tridentate hydrazone-ibuprofen scaffold (**L_3** and **L_4**) hinders the placement of chloride ion at the corner of the plane as a consequence of unequal ligand-field strength and (iii) better structural flexibility of ibuprofen that contributes toward reorganisation of square planar geometry for accommodating the Cl^- ion within the coordination sphere.

Usually, it is observed that square planar geometry exhibits axial symmetry through stacking of structural planes of Cu(II) complexes. To ascertain this aspect, ESR data are used for the calculation of *G* parameter from the following equation:

$$G = (g_{||} - 2.0023)/(g_{\perp} - 2.0023)$$

This value is found to be > 4, indicating the absence of magnetic interaction between successive square planes of these complexes [54]. Thus, it can be argued that the geometry of these complexes is substantially distorted form idealised square planar structure, which results in negligible axial interactions for these complexes. Moreover, these complexes are quite stable in solution as evident from spectral studies and this aspect may be benefical for the evaluation of acticancer activity aganist different cancer cell lines.

3.5. Anticancer activity

In vitro anti-proliferative activity of **L_1**–**L_4** and their Cu(II) complexes is evaluated against human lung carcinoma (A549), human colon cancer (HCT116) and breast cancer (MDA MB-231) cell lines by MTT assay after 24 h. Different concentrations of ligands and complexes (0.1, 1, 10 and 100 μM) are employed for the estimation of IC_{50} value with DMSO as control.

Hydrazones of diclofenac and ibuprofen (**L_1**–**L_4**) exhibit concentration dependent cytotoxicity where % cell viability increases with concomitant decrease in the concentration of these ligands (Figure S13). Although **L_1**–**L_4** are active against these cell lines, they exhibit better cytotoxicity against breast cancer cell line and the order of activity is found to be MDA MB-231 > A549 > HCT116 for these ligands. Among ligands, imidazole-based conjugates (**L_2** and **L_4**) are found to be more potent than pyridine-hydrazones. This feature is also reflected form their IC_{50} values (Table 3) where significantly lowered values are observed for MDA MB-231. Based on these results, the order of cytotoxicity for hydrazone-NSAID conjugates is found to be **L_4** > **L_2** > **L_3** > **L_1**. Interestingly, these values are significantly lower than those reported for diclofenac and ibuprofen against different cancer cell lines [55–58]. The exceptionally higher toxicity for **L_1**–**L_4** may be attributed to synergistic association of the hydazone linkage and NSAID that ultimately improves the therapeutic potential of hydrazine–NSAID scaffold. It also implies that conjugation of

Table 3. IC_{50} (μM) values[$] for L_1 to L_4 and **Cu-1** to **Cu-4** against (a) A549 (b) HCT116 and (c) MDA MB-231.

	Cell line		
Compound	A549	HCT116	MDA MB-231
L_1	67.90 ± 1.83	73.33 ± 4.18	24.11 ± 1.38
L_2	51.94 ± 1.71	61.53 ± 2.78	14.78 ± 1.17
L_3	44.84 ± 1.65	58.62 ± 5.50	6.74 ± 0.83
L_4	26.05 ± 1.41	60.34 ± 2.65	2.26 ± 0.35
Cu-1	18.36 ± 1.26	49.74 ± 2.68	6.62 ± 0.82
Cu-2	27.58 ± 1.44	55.06 ± 2.98	3.96 ± 0.59
Cu-3	37.38 ± 1.57	56.90 ± 3.39	3.87 ± 0.58
Cu-4	26.91 ± 1.43	45.10 ± 3.24	3.38 ± 0.53

[$]All the data are presented as mean ± SD of three independent experiments at $p < 0.001$, indicating statistically significant differences compared to the control untreated cells.

NSAID with hydrazone has resulted in the formation of bioactive species with enhaced anticancer activity.

From the cell viability studies of complexes, it is observed that some of them complexes exhibit enhanced anticancer activity as compared to L_1–L_4. For example, **Cu-1** to **Cu-4** possess better cytotoxicity against MDA MB-231 while there seems to be almost negligible effect of complexation for these ligands against A549 and HCT116. Among these complexes, **Cu-4** is found to be more toxic than other complexes while all these complexes are more active toward A549 cell line than other two cell lines. The order of activity for complexes is **Cu-4** > **Cu-3** > **Cu-1** > **Cu-2** while for different cell lines, **Cu-4** exhibits significant cytotoxicity against MDA MB-231. Moreover, IC_{50} values estimated from one-way ANOVA analysis suggest that Cu(II) complexes possess lower or almost similar toxicity than their corresponding ligands (Table 3). Interestingly, excellent anticancer activity is observed for these complexes against MDA MB-231 as compared to other cell lines at substantially lower concentrations. Although **Cu-1** and **Cu-2** exhibit lower IC_{50} values as compared to L_1 and L_2, substantially decreased lethal concentration for 50% killing is noted for **Cu-3** and **Cu-4** against breast MBA MB-231. Strikingly, **Cu-1** and **Cu-2** also possess similar activity against A549 and HCT116 at significantly higher IC_{50} values. Thus, it may be argued that Cu(II) complexes of diclofenac-hydrazones are more potent anticancer agents than ibuprofen conjugates.

To assess the potentiality of synthesized complexes, the IC_{50} values of these complexes are compared with different metal complexes of diclofenac, ibuprofen and hydrazones (Table 4). It is interesting to note that **Cu-1** to **Cu-4** exhibit significant toxicity at substantially lower IC_{50} value as compared to diclofenac [57], ibuprofen [58] and their corresponding metal complexes [33, 59–61]. For example, Cu(II) complexes of diclofenac [33] and ibuprofen [59] possesses moderate-to lower activity against colon cancer while their Ag(I) complexes [60,61] are comparatively less toxic towards HT29 and MCF-7. In our case, excellent activity is observed against breast cancer cell line whereas moderate cytotoxic nature is noted with HCT115. Moreover, the synthesized ibuprofen-Cu(II)-conjugates (**Cu-3** and **Cu-4**) are less toxic with considerably higher IC_{50} values against colon cancer as compared to Sn-ibuprofen complex $\{[Me_2Sn(ibuprofen)]_2O_2\}$ [62]. However, diclofenac and ibuprofen conjugated cisplatin scaffold exhibit significant antitumor activity against HCT116 and MDA-MB-21 with ibuprofen complex possessing extremely lower IC_{50} value,

Table 4. IC_{50} (μM) values of metal complexes of NSAID against cancer cell lines.

Compound	Cell line	IC_{50}	Reference
Diclofenac	MDA-MB-231	139	[57]
	A549	> 100	
	HCT115	169	[58]
Ibuprofen	MDA-MB-231	968	
	A549	789	
	HCT115	448	
$[Cu(diclofenac)_2(H_2O)_2]$	SW620	30	[33]
	HT29	20	
$[Cu(ibuprofen)_2(H_2O)_2]$	HT144	113.24	[59]
[Ag(diclofenac)n]	HT29	53.20	[60]
	MCF-7	26.64	
$[Ag_2(\mu\text{-diclofenac})_4(4\text{-pic})_2]$	HT29	45.36	[61]
	MCF-7	26.15	
$\{[Me_2Sn(ibuprofen)]_2O_2\}$	HCT15	2.19	[62]
$[Pt(NH_3)_2(H_2O)_2(diclofenac)_2]$	HCT116	2.5	[63]
	MDA-MB-231	20.1	
$[Pt(NH_3)_2(H_2O)_2(ibuprofen)_2]$	HCT116	0.22	
	MDA-MB-231	1.05	
Cisplatin	A549	52	[64]
	MDA-MB-231	63-66	
	HCT116	4.22	
Cu-1	MDA-MB-231	6.62	Present work
	A549	18.36	
	HCT115	49.74	
Cu-2	MDA-MB-231	3.97	
	A549	27.58	
	HCT115	55.06	
Cu-3	MDA-MB-231	3.87	
	A549	37.38	
	HCT115	56.90	
Cu-4	MDA-MB-231	3.38	
	A549	26.91	
	HCT115	45.10	

probably due to synergistic association of cisplatin and NSAID [63]. The anticancer activity of these complexes is also compared with Cu-hydrazone complexes [65–70]. From this assessment, it is observed that **Cu-1** to **Cu-4** possess substantially lower IC_{50} values which further corroborate our hypothesis that hydrazone linkage significantly contributes toward improved anticancer activity of parent ligating system. For example, Cu(II)-2,10-oxybenzaldehyde benzhydrazonato complex exhibits excellent anticancer activity against liver cancer cell line HepG2 [66] while copper complex of *N*′-((E)-1-(pyridin-2-yl)ethylidene)adamantine-1-carbohydrazide displays considerably lower IC_{50} value against A549 [70]. However, comparatively lower activity is observed for the synthesized hydrazone complexes against A549 whereas they display substantial anti-proliferative activity against breast cancer cell line. Interestingly, **Cu-1** to **Cu-4** are found to be almost 15 times more potent than cisplatin, a clinically approved anticancer drug [64]. Moreover, these complexes possess substancially lower IC_{50} values (3.38–6.62 μM) as compared to cisplatin. Such behavior may be attributed to the combined effect of both NSAID and hydrazone motif that significantly improve the antitumor activity of the conjugates. Thus, it may be concluded that NSAID-hydrazone-copper scaffold indeed exerts beneficial anticancer activity in a synergistic manner and possess excellent potentiality as anticancer drug.

4. Conclusions

Four Cu(II)-NSAID-hydrazone complexes constructed from anti-inflammatory drugs like diclofenac and ibuprofen are synthesized and evaluated for their anticancer activity. Hydrazone ligands are found to exhibit *cis-trans* isomerism (rotamers) while their complexes exhibit two different types of stoichiometric compounds. Although a square geometry is formed with these complexes, bis-complexes are formed with diclofenac possessing bi-dentate nature while the corresponding ibuprofen complexes contain a tridentate hydrazone binding with ancillary Cl^- thereby formaing a four-coordinate structure. The electrochemical studies indicate an irreversible one-electron Cu(II)/Cu(I) redox couple at more positive potentials. EPR measurements suggest the appreciable covalency in M–L bonding with significant distortion in square-planar geometry, implying the influence of structural orientation of hydrazones. The excellent anticancer activity of these complexes with significantly lower IC_{50} value probably arises from the synergistic association of NSAID-hydrazone-Cu(II) linkage. Thus, it may be argued that conjugation of hydrazone with NSAID and their complexation with less toxic metal ion may be regarded as alternative strategy for desiging of potent anticaner agents with better activity at substancially lower concentration as compared to cis-platin.

Disclosure statement

No potential conflict of interest was reported by the authors.

Acknowledgements

The authors are thankful to Principal, Abasaheb Garware College for the kind support. The authors express deep sense of gratitude to Dr. Shyamal Chattopadhyay, BESU, Kolkata, for analytical measurements.

ORCID

Soumya Basu http://orcid.org/0000-0002-1726-0154
Rajeev Chikate http://orcid.org/0000-0002-6312-0582

References

[1] L. Simmons, D. Wagner, K. Westover. *Clin. Infect. Dis.*, **31**, S211 (2000).
[2] (a) C.K.S. Ong, P. Lirk, C.H. Tan, R.A. Seymour. *Clin. Med., Res.*, **5**, 19 (2007). (b) R.S. Hoffman, R. Braga-Mele, K. Donaldson, G. Emerick, B. Henderson, M. Kahook, N. Mamalis, K.M. Miller, T. Realini, N.H. Shorstein, R.K. Stiverson, B. Wirostko. *J. Cataract Refract. Surg.*, **49**, 1368 (2016).
[3] (a) L.J. Crofford. *Arthritis Res. Ther.*, **15**, S2 (2013). (b) V.A. Guilherme, L.N.M. Ribeiro, A.C.S. Alcântara, S.R. Castro, G.H.R. da Silva, C.G. da Silva, M.C. Breitkreitz, J. Clemente-Napimoga, C.G. Macedo, H.B. Abdalla, R. Bonfante, C.M.S. Cereda, E. de Paula. *Sci. Rep.*, **9**, 11160 (2019). (c) O. Akgul, L. Di Cesare Mannelli, D. Vullo, A. Angeli, C. Ghelardini, G. Bartolucci, A. Saleh Alfawaz Altamimi, A. Scozzafava, C.T. Supuran, F. Carta. *J. Med. Chem.*, **61**, 4961 (2018).
[4] (a) P. Emery. *Drugs Today (Barc)*, **35**, 267 (1999). (b) Z. Zhang, F. Chen, L. Shang. *Cancer Manag. Res.*, **10**, 4631 (2018).

[5] (a) P.N.P. Rao, E.E. Knaus.Prostate Int, **7**, 156(2019). (b) E.D. Arisan, R.O. Akar, O. Rencuzogullari, P.O. Yerlikaya, A.C. Gurkan, B. Akın, E. Dener, E. Kayhan, N.P. Unsal. *Prostate Int.*, **7**, 156 (2019).
[6] E. Ricciotti, G.A. FitzGerald. *Arterioscler. Thromb. Vasc. Biol.*, **31**, 986 (2011).
[7] M.E. Turini, R.N. DuBois. *Annu. Rev. Med.*, **53**, 35 (2002).
[8] (a) L. Hilovská, R. Jendželovský, P. Fedoročko. *Mol. Clin. Oncol.*, **3**, 3 (2015). (b) G.J. Tsioulias, M.F. Go, B. Rigas. *Curr. Pharmacol. Rep.*, **1**, 295 (2015).
[9] D.H. Woo, I.-S. Han, G. Jung. *Life Sci.* , **75**, 2439 (2004).
[10] D.J.A. de Groot, E.G.E. de Vries, H.J.M. Groen, S. de Jong. *Crit. Rev. Oncol. Hematol.* , **61**, 52 (2007).
[11] E. Gurpinar, W.E. Grizzle, G.A. Piazza. *Front. Oncol.*, **3**, 181 (2013).
[12] E.R. Rayburn, S.J. Ezell, R. Zhang. *Mol. Cell. Pharmacol.*, **1**, 29 (2009).
[13] P. Pantziarka, V. Sukhatme, G. Bouche, L. Meheus, V.P. Sukhatme. *Ecancermedicalscience*, **10**, 610 (2016).
[14] M.S.M. Al-Nimer, H.G. Hameed, M.M. Mahmood. *Saudi Pharm. J.*, **23**, 483 (2015).
[15] C.N. Banti, A.D. Giannoulis, N. Kourkoumelis, A.M. Owczarzak, M. Kubicki, S.K. Hadjikakou. *Dalton Trans.*, **43**, 6848 (2014).
[16] F. Albano, A. Arcucci, G. Granato, S. Romano, S. Montagnani, E. De Vendittis, M.R. Ruocco. *Biochimie*, **95**, 934 (2013).
[17] H. Endo, M. Yano, Y. Okumura, H. Kido. *Cell Death Dis.*, **5**, e1027 (2014).
[18] S. Xiang, Z. Sun, Q. He, F. Yan, Y. Wang, J. Zhang. *Med. Oncol.*, **27**, 379 (2010).
[19] (a) D. Nie, K.V. Honn. *Cell. Mol. Life Sci.*, **59**, 799 (2002). (b) H.Y. Khan, S. Tabassum, F. Arjmand. *RSC Adv.*, **10**, 166 (2020). (c) A.M. Gouda, E.A. Beshr, F.A. Almalki, H.H. Halawah, B.F. Taj, A.F. Alnafaei, R.S. Alharazi, W.M. Kazi, M.M. AlMatrafi. *Bioorg. Chem.*, **92**, 103224 (2019).
[20] V.S. Neergheen, T. Bahorun, E.W. Taylor, L.S. Jen, O.I. Aruoma. *Toxicology*, **278**, 229 (2010).
[21] C. Gunaydin, S.S. Bilge. *Eurasian J. Med.*, **50**, 116 (2018).
[22] A. Zarghi, S.A. Iran. *J. Pharm. Res.*, **10**, 655 (2011).
[23] R. Hanif, A. Pittas, Y. Feng, M.I. Koutsos, L. Qiao, L. Staiano-Coico, S.I. Shiff, B. Rigas. *Biochem. Pharmacol.*, **52**, 237 (1996).
[24] A. Upadhyay, A. Amanullah, D. Chhangani, V. Joshi, R. Mishra, A. Mishra. *Mol. Neurobiol.*, **53**, 6968 (2016).
[25] A.C. Chai, A.L. Robinson, K.X. Chai, L. Chen. *BMC Cancer*, **15**, 1025 (2015).
[26] R.E. Harris, J. Beebe-Donk, H. Doss, D.B. Doss. *Oncol. Rep.*, **13**, 559 (2005).
[27] F.P. Intini, J. Zajac, V. Novohradsky, T. Saltarella, C. Pacifico, V. Brabec, G. Natile, J. Kasparkova. *Inorg. Chem.*, **56**, 1483 (2017).
[28] (a) D.K. Demertzi, D.H. Litina, M. Staninska, A. Primikiri,C. Kotoglou, M.A. Demertzis. *J. Eng. Inhib. Med. Chem.*, **24**, 742 (2009). (b) A. Curci, N. Denora, R.M. Iacobazzi, N. Ditaranto, J.D. Hoeschele, N. Margiotta, G. Natile. *Inorg. Chim. Acta*, **472**, 221 (2018). (c) C.N. Banti, A.G. Hatzidimitriou, N. Kourkoumelis, S.K. Hadjikakou. *J. Inorg. Biochem.*, **194**, 7 (2019).
[29] H.A. Ali, S.N. Omar, M.D. Darawsheh, H. Fares. *J. Coord. Chem.*, **69**, 1110 (2016).
[30] M. Roch-Arveiller, D.P. Huy, L. Maman, J.-P. Giroud, J.R.J. Sorenson. *J.R. Sorenson. Biochem. Pharmacol*, **39**, 569 (1990).
[31] D. Mahendiran, R.S. Kumar, A.K. Rahiman. *Mater. Sci. Eng. C Mater. Biol. Appl.*, **76**, 601 (2017).
[32] C. Leung, S. Lin, H. Zhong, M. Dik-Lung. *Chem. Sci.*, **6**, 871 (2015).
[33] S. Sayen, A. Carlier, M. Tarpin, E. Guillon. *J. Inorg. Biochem.*, **120**, 39 (2013).
[34] A. Hussain, M.F. AlAjmi, M.T. Rehman, S. Amir, F.M. Husain, A. Alsalme, M.A. Siddiqui, A.A. Al Khedhairy, R.A. Khan. *Sci. Rep.*, **9**, 5237 (2019).
[35] M.A. Shaheen, S. Feng, M. Anthony, M.N. Tahir, M. Hassan, S. Seo, S. Ahmad, M. Iqbal, M. Saleem, C. Lu. *Molecules*, **24**, 1237 (2019).
[36] R.H. Wiley, R.L. Clevenger. *J. Med. Chem.*, **5**, 1367 (1962).
[37] A. Kajal, S. Bala, N. Sharma, S. Kamboj, V. Saini. *Int. J. Med. Chem.*, **2014**, 761030 (2014).
[38] D. Sriram, P. Yogeeswari, R.V. Devakaram. *Bioorg. Med. Chem.*, **14**, 3113 (2006).
[39] V. Sharma, M.S.Y. Khan. *Pharmazie*, **58**, 99 (2003).
[40] D. Mahendiran, S. Amuthakala, N.S.P. Bhuvanesh, R.S. Kumar, A.K. Rahiman. *RSC Adv.*, **8**, 16973 (2018).

[41] R.C. Chikate, A.R. Belapure, S.B. Padhye, D.X. West. *Polyhedron*, **24**, 889 (2005).
[42] C.P. Pradeep, P.S. Zacharias, S.K. Das. *J. Chem. Sci.*, **117**, 133 (2005).
[43] O.O. Abosede, N.A. Vyas, S.B. Singh, A.S. Kumbhar, A. Kate, A.A. Kumbhar, A. Khan, A. Erxleben, P. Smith, C. Kock, F. Hoffmann, J.A. Obaleye. *Dalton Trans.*, **45**, 3003 (2016).
[44] S. Mondal, S. Naskar, A.K. Dey, E. Sinn, C. Eribal, S.R. Herron, S.K. Chattopadhyay. *Inorg. Chim. Acta*, **398**, 98 (2013).
[45] W. Kaim, M. Moscherosch. *Faraday Trans.*, **87**, 3185 (1991).
[46] M. Nandy, D.L. Hughes, G.M. Rosair, R. Kumar, B. Singh, S. Mitra. *J. Coord. Chem.*, **67**, 3335 (2014).
[47] D. Mahendiran, P. Gurumoorthy, K. Gunasekaran, R.S. Kumar, A.K. Rahiman. *New J. Chem.*, **39**, 7895 (2015).
[48] C. Miller, J. Fajardo, W.E. Antholine, D.R. McMillin. *Anal. Biochem.*, **227**, 69 (1995).
[49] J. Ravichandran, P. Gurumoorthy, M.A.I. Musthafa, A.K. Rahiman. *Spectrochim Acta A Mol. Biomol. Spectrosc.*, **133**, 785 (2014).
[50] J.C. Vedrine, E.G. Derouane, Y.B. Taarit. *J. Phys. Chem.*, **78**, 531 (1974).
[51] B.J. Hathaway, D.E. Billing. *Coord. Chem. Rev.*, **5**, 143 (1970).
[52] B.J. Hathway. *Struct. Bond*, **14**, 49 (1973).
[53] R. C. Chikate, S. B. Padhye. *Polyhedron*, 24, 1698 (2005).
[54] M.S.S. Babu, P.G. Krishna, K.H. Reddy, G.H. Philip. *Main Group Chem.*, **8**, 101 (2009).
[55] (a) L.J. Hixson, D.S. Alberts, M. Krutzsch, J. Einsphar, K. Brendel, P.H. Gross, N.S. Paranka, M. Baier, S. Emerson, R. Pamukcu, R.W. Burt. *Cancer Epidemiol. Biomark. Prevent.*, **3**, 433 (1994). (b) C.N. Banti, S.K. Hadjikakou. *Eur. J. Inorg. Chem.*, **2016**, 3048 (2016).
[56] (a) M. Barbaric, M. Kralj, M. Marjanovic, I. Husnjak, K. Pavelic, J.F. Gricic, D. Zorc, B. Zorc. *Eur. J. Med. Chem.*, **42**, 20 (2007). (b) M. Chattopadhyay, R. Kodela, N. Nath, Y.M. Dastagirzada, C.A. Velazquez-Martinez, D. Boring, K. Kash. *Biochem. Pharmacol.*, **83**, 715 (2012).
[57] (a) K.M. Oliveira, J. Honorato, G.R. Gonçalves, M.R. Cominetti, A.A. Batista, R.S. Correa. *Dalton Trans.*, **49**, 12643 (2020); (b) C.N. Banti, S.K. Hadjikakou. *Eur. J. Inorg. Chem.*, **2016**, 3048 (2016). (c) G.A. Piazza, A.B. Keeton, H.N. Tinsley, J.D. Whitt, B.D. Gary, B. Mathew, R. Singh, W.E. Grizzle, R.C. Reynolds. *Pharmaceuticals*, **3**, 1652 (2010).
[58] (a) M. Chattopadhyay, R. Kodela, N. Nath, Y.M. Dastagirzada, C.A.V. Martınez, D. Boring, K. Kash. *Biochem. Pharmacol.*, **83**, 715 (2012). (b) B.Z. Wegrzynska, M. Kawalec, I. Bosek, M. Juzwa, G. Adamus, A. Rusin, P. Filipczak, M.G. Kosinska, K. Wolanska, Z. Krawczyk, P. Kurcok. *Eur. J. Med. Chem.*, **45**, 1833 (2010).
[59] S. Kumar, S. Garg, R.P. Sharma, P. Venugopalan, L. Tenti, V. Ferretti, L. Nivelle, M. Tarpin, E. Guillon. *New J. Chem.*, **41**, 8253 (2017).
[60] A. Altay, S. Caglar, B. Caglar. *Arch. Physiol. Biochem.*, **1**, 11 (2019).
[61] A. Altay, S. Caglar, B. Caglar, O. Sahin. *Polyhedron*, **151**, 160 (2018).
[62] R. Kumari, S. Banerjee, P. Roy, M. Nath. *Appl. Organomet. Chem.*, **34**, e5283 (2020).
[63] W. Neumann, B.C. Crews, L.J. Marnett, E. Hey-Hawkins. *ChemMedChem*, **9**, 1150 (2014).
[64] (a) K.S. Lovejoy, M. Serova, I. Bieche, S. Emami, M.D. Incalci, M. Broggini, E. Erba, C. Gespach, E. Cvitkovic, S. Faivre, E. Raymond, S.J. Lippard. *Mol. Cancer Therapeutics*, **10**, 1709 (2011). (b) C.H. Dai, J. Li, P. Chen, H.G. Jiang, M. Wu, Y.C. *Chen. J. Biomed. Sci.*, **22**, 1 (2015). (c) C.H. Ng, S.M. Kong, Y.L. Tiong, M.J. Maah, N. Sukram, M. Ahmad, A.S.B. Kho. *Metallomics*, **6**, 892 (2014).
[65] K. Hu, F. Li, Z. Zhang, F. Liang. *New J. Chem.*, **41**, 2062 (2017).
[66] M. Cindrić, A. Bjelopetrović, G. Pavlović, V. Damjanović, J. Lovrić, D. Matković-Čalogović, V. Vrdoljak. *New J. Chem.*, **41**, 2425 (2017).
[67] B. Deka, T. Sarkar, S. Banerjee, A. Kumar, S. Mukherjee, S. Deka, K.K. Saikia, A. Hussain. *Dalton Trans.*, **46**, 396 (2017).
[68] K.E. Prosser, S.W. Chang, F. Saraci, P.H. Le, C.J. Walsby. *J. Inorg. Biochem.*, **167**, 89 (2017).
[69] J. Zhao, S. Zhi, H. Yu, R. Mao, J. Hu, W. Song, J. Zhang. *RSC Adv.*, **7**, 51162 (2017).
[70] V.M. Leovac, M.V. Rodić, L.S. Jovanović, M.D. Joksović, T. Stanojković, M. Vujčić, D. Sladić, V. Marković, L.S. Vojinović-Ješić. *Eur. J. Inorg. Chem.*, **2015**, 882 (2015).